Polarization independent VOA based on dielectrically stretched liquid crystal droplet

Su Xu,[1] Hongwen Ren,[2] Jie Sun,[1] and Shin-Tson Wu[1,*]

[1]*CREOL, The College of Optics and Photonics, University of Central Florida, Orlando, Florida 32816, USA*
[2]*Department of Polymer Nano-Science and Engineering, Chonbuk National University, Chonju, Chonbuk, 561-756 Republic of South Korea*
[*]*swu@mail.ucf.edu*

Abstract: A polarization independent variable optical attenuator (VOA) based on a dielectrically stretched liquid crystal (LC) droplet is demonstrated. In the voltage-off state, the proposed VOA has the smallest attenuation. As voltage increases, the LC droplet is stretched by a dielectrophoretic force, which gradually deflects the beam leading to an increased attenuation. Such a VOA can cover the entire C-Band. At λ = 1550 nm, the following results are obtained: dynamic range ~32 dB, insertion loss ~0.7 dB, polarization dependent loss ~0.3 dB, and response time ~20 ms.

OCIS codes: (130.4815) Optical switching devices; (230.2090) Electro-optical devices.

References and links

1. H. Schenk, P. Dürr, D. Kunze, H. Lakner, and H. Kück, "A resonantly excited 2D-micro-scanning-mirror with large deflection," Sens. Actuators A Phys. **89**(1–2), 104–111 (2001).
2. S. H. Hung, H. T. Hsieh, and G. D. J. Su, "An electro-magnetic micromachined actuator monolithically integrated with a vertical shutter for variable optical attenuation," J. Micromech. Microeng. **18**(7), 075003 (2008).
3. L. Zhu, Y. Huang, and A. Yariv, "Integrated microfluidic variable optical attenuator," Opt. Express **13**(24), 9916–9921 (2005).
4. M. I. Lapsley, S. C. S. Lin, X. Mao, and T. J. Huang, "An in-plane, variable optical attenuator using a fluid-based tunable reflective interface," Appl. Phys. Lett. **95**(8), 083507 (2009).
5. R. A. Soref and D. H. McMahon, "Total switching of unpolarized fiber light with a four-port electro-optic liquid-crystal device," Opt. Lett. **5**(4), 147–149 (1980).
6. N. A. Riza and S. A. Khan, "Liquid-crystal-deflector based variable fiber-optic attenuator," Appl. Opt. **43**(17), 3449–3455 (2004).
7. Y. H. Fan, Y. H. Lin, H. Ren, S. Gauza, and S. T. Wu, "Fast-response and scattering-free polymer network liquid crystals for infrared light modulators," Appl. Phys. Lett. **84**(8), 1233–1235 (2004).
8. F. Du, Y. Q. Lu, H. Ren, S. Gauza, and S. T. Wu, "Polymer-stabilized cholesteric liquid crystal for polarization-independent variable optical attenuator," Jpn. J. Appl. Phys. **43**(10), 7083–7086 (2004).
9. Y. Q. Lu, F. Du, Y. H. Lin, and S. T. Wu, "Variable optical attenuator based on polymer stabilized twisted nematic liquid crystal," Opt. Express **12**(7), 1221–1227 (2004).
10. Y. H. Wu, Y. H. Lin, Y. Q. Lu, H. Ren, Y. H. Fan, J. Wu, and S. T. Wu, "Submillisecond response variable optical attenuator based on sheared polymer network liquid crystal," Opt. Express **12**(25), 6382–6389 (2004).
11. K. Takizawa, K. Kodama, and K. Kishi, "Polarization-independent optical fiber modulator by use of polymer-dispersed liquid crystals," Appl. Opt. **37**(15), 3181–3189 (1998).
12. K. M. Chen, H. Ren, and S. T. Wu, "PDLC-Based VOA with a small polarization dependent loss," Opt. Commun. **282**(22), 4374–4377 (2009).
13. W. Hu, A. Srivastava, F. Xu, J. T. Sun, X. W. Lin, H. Q. Cui, V. Chigrinov, and Y. Q. Lu, "Liquid crystal gratings based on alternate TN and PA photoalignment," Opt. Express **20**(5), 5384–5391 (2012).
14. W. Hu, A. K. Srivastava, X. W. Lin, X. Liang, Z. J. Wu, J. T. Sun, G. Zhu, V. Chigrinov, and Y. Q. Lu, "Polarization independent liquid crystal gratings based on orthogonal photoalignments," Appl. Phys. Lett. **100**(11), 111116 (2012).
15. J. Yan, Y. Li, and S. T. Wu, "High-efficiency and fast-response tunable phase grating using a blue phase liquid crystal," Opt. Lett. **36**(8), 1404–1406 (2011).
16. C. G. Tsai and J. A. Yeh, "Circular dielectric liquid iris," Opt. Lett. **35**(14), 2484–2486 (2010).
17. H. Ren, S. Xu, and S. T. Wu, "Deformable liquid droplets for optical beam control," Opt. Express **18**(11), 11904–11910 (2010).

#169848 - $15.00 USD Received 4 Jun 2012; revised 1 Jul 2012; accepted 5 Jul 2012; published 11 Jul 2012

18. H. Ren, S. Xu, D. Ren, and S. T. Wu, "Novel optical switch with a reconfigurable dielectric liquid droplet," Opt. Express **19**(3), 1985–1990 (2011).
19. J. L. Jackel, S. Hackwood, and G. Beni, "Electrowetting optical switch," Appl. Phys. Lett. **40**(1), 4–5 (1982).
20. S. A. Reza and N. A. Riza, "A liquid lens-based broadband variable fiber optical attenuator," Opt. Commun. **282**(7), 1298–1303 (2009).
21. C. U. Murade, J. M. Oh, D. van den Ende, and F. Mugele, "Electrowetting driven optical switch and tunable aperture," Opt. Express **19**(16), 15525–15531 (2011).
22. C. Karuwan, K. Sukthang, A. Wisitsoraat, D. Phokharatkul, V. Patthanasettakul, W. Wechsatol, and A. Tuantranont, "Electrochemical detection on electrowetting-on-dielectric digital microfluidic chip," Talanta **84**(5), 1384–1389 (2011).
23. G. G. Hougham, P. E. Cassidy, K. Johns, and T. Davidson, *Fluoropolymers 2: Properties* (Plenum Press, New York, 1999).
24. H. Ren, S. Xu, and S. T. Wu, "Voltage-expandable liquid crystal surface," Lab Chip **11**(20), 3426–3430 (2011).
25. P. Penfield and H. A. Haus, *Electrodynamics of Moving Media* (Cambridge, MIT, 1967).
26. M. van Buren and N. A. Riza, "Foundations for low-loss fiber gradient-index lens pair coupling with the self-imaging mechanism," Appl. Opt. **42**(3), 550–565 (2003).
27. D. K. Yang and S. T. Wu, *Fundamentals of Liquid Crystal Devices* (Wiley, 2006).
28. H. Ren, H. Xianyu, S. Xu, and S. T. Wu, "Adaptive dielectric liquid lens," Opt. Express **16**(19), 14954–14960 (2008).
29. S. Xu, Y. J. Lin, and S. T. Wu, "Dielectric liquid microlens with well-shaped electrode," Opt. Express **17**(13), 10499–10505 (2009).

1. Introduction

Variable optical attenuators (VOAs) have been widely used in fiber-optic communication, photonic signal processing, sensing as well as testing instruments. Several approaches have been proposed in the past years. MEMS VOAs [1,2] have a microsecond response time, but the microshutters (or the reflective micromirrors) bring up the reliability issue and it is difficult to integrate with other planar optical elements. Microfluidic VOAs alter the refractive index of the fluid within microchannels to control the beam reflection or refraction [3,4]. They are attractive for easy in-plane integration and biochemical sensing, but the inconvenient driving scheme and fabrication procedures (one step or multistep photolithography and soft lithography) limit their applications. VOAs based on liquid crystals (LCs) [5–15], dielectrophoretic (DEP) effect [16–18] and electrowetting [19–21] have no mechanical moving parts. Nematic liquid crystal VOAs have advantages in low cost, low optical loss, low power consumption, and grayscale capability, but the response time is relatively slow [5,6] and most of them are polarization dependent. Polymer-network liquid crystal (PNLC)-based VOAs exhibit a fast response time at room temperature, but the tradeoffs are increased operating voltage and light scattering [7–9]. On the other hand, sheared PNLC has lower driving voltage and negligible light scattering, but the mechanical shearing process adds fabrication complexity [10]. Polymer-dispersed liquid crystal, in principle, is polarization independent, but to keep large dynamic range and small polarization dependent loss (PDL) simultaneously is a challenging task [11,12]. VOAs based on LC grating have also been demonstrated. With conventional nematic LCs, the diffraction efficiency is usually low (~30%) and the response time is relatively slow (>10 ms) [13,14]. Polymer-stabilized blue phase LC grating has a high diffraction efficiency (~40%) and submillisecond response time, but the operating voltage is fairly high [15]. Most DEP [16–18] and electrowetting [19–21] VOAs only work in the visible spectral region. For fiber communications, an electrowetting lens-based broadband VOA has been reported [20]. This device adopts an electronically controlled optical wedge to vary the tilt angle of the output beam which in turn changes the coupling efficiency. It shows broadband operation at C-Band, ~40 dB dynamic range, 0.3 dB PDL and <100 ms switching time, but the insertion loss is ~4.3 dB.

In this paper, we demonstrate a VOA based on dielectrically stretched LC droplet for C-Band operation. It utilizes a stretchable LC droplet to deflect the incident beam. In the voltage-off state (V = 0), the beam passes through the VOA without any deflection. As the voltage increases, the LC droplet surface is gradually stretched by the dielectric force, which

#169848 - $15.00 USD Received 4 Jun 2012; revised 1 Jul 2012; accepted 5 Jul 2012; published 11 Jul 2012

deflects the incident beam away leading to attenuated transmission. Such a VOA can cover the entire C-Band (1530-1560 nm) operation. Specifically at λ = 1550 nm, we obtain ~32 dB dynamic range, ~0.7 dB insertion loss, ~0.3 dB PDL and ~20 ms response time. The peak operating voltage is ~40V_{rms}.

2. Device structure and operation principles

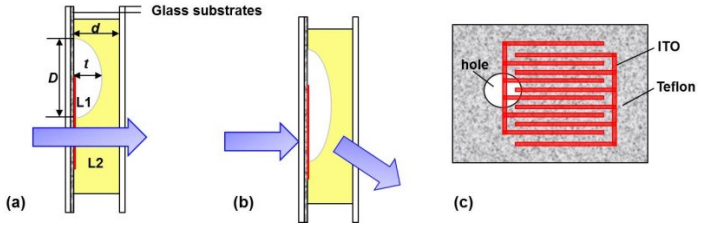

Fig. 1. (a) Side-view structure of the VOA at V = 0, (b) V>0, and (c) the layout of the interdigitated ITO electrode and Teflon layer on the bottom substrate (The hole size and the width of ITO stripes are not drawn by scale.)

Figure 1(a) shows the side-view structure of the proposed device. Two liquids (L1 and L2) are sandwiched between two glass substrates. L1 forms a droplet on the bottom substrate and L2 fills the surrounding space. Detailed layout of the bottom substrate is shown in Fig. 1(c). Its inner surface is coated with interdigitated indium tin oxide (ITO) electrodes (marked as red in Fig. 1), on the top of which is a thin polyimide layer (PI2556, HD Microsystems, surface tension γ_P~40 mN/m, ~1 μm thickness, not shown in Fig. 1) and a hole-patterned Teflon layer (400S1-100-1, DuPont, γ_T ~19 mN/m, ~1 μm thickness, marked as gray in Fig. 1). These two layers not only provide a suitable contact angle for the droplet [22,23], but also prevent the carrier injection into the cell. Therefore, our device is free from the concern of charge effect. The hole partially contacts with the electrodes, pinning down the droplet position. Due to its simple structure and easy fabrication process, such a VOA's cost should be relatively low.

To keep operation voltage as low as possible, liquid L1 should have a large dielectric constant and a low surface tension [24]. Here we chose Merck nematic LC mixture ZLI-4389 as L1. Its physical properties are listed as follows: $\varepsilon_{//} = 56$, $\Delta\varepsilon = 45.6$, γ~38mN/m, $\langle n \rangle$~1.58, and ρ~0.98 g/m^3. L2 is silicone oil with ε~2.9, γ~21 mN/m, n~1.4, and ρ~0.97 g/cm^3. These two liquids are immiscible and match well in density. At the rest state, the aperture (D) and apex distance (t) of the droplet is ~450 μm and ~200 μm, respectively, and the cell gap (d) is ~270 μm, as labeled in Fig. 1(a). The width and gap of the interdigitated ITO electrodes are both 10 μm.

The incident beam from a single-mode fiber (SMF) is intentionally adjusted to pass near the droplet's border, where a maximum change in the droplet's surface occurs, as Fig. 1(a) shows. At V = 0, the droplet shrinks in the hole with the smallest surface-to-volume ratio. The incident beam stays aligned with the output SMF for maximum coupling and minimum attenuation. When a voltage is applied to the bottom electrodes, a nonuniform lateral electric field is generated across the ITO stripes and a dielectric force is exerted on the liquid-liquid interface, According to Kelvin's theory, the dielectric force density can be expressed as [25]:

$$\vec{F} = \frac{\varepsilon_0}{2}(\varepsilon_1 - \varepsilon_2)\nabla(E \bullet E), \qquad (1)$$

where ε_0 represents the permittivity of free space, ε_1 and ε_2 denote the dielectric constants of L1 and L2, respectively, and E denotes the electric field on curved droplet. Since the LC molecules on the droplet border are reoriented by fringing field, the dielectric constant on the border should be close to $\varepsilon_{//} = 56$, which is much larger than that of the silicone oil. Therefore,

#169848 - $15.00 USD Received 4 Jun 2012; revised 1 Jul 2012; accepted 5 Jul 2012; published 11 Jul 2012

the droplet border bears the strongest dielectric force along the ITO stripe direction. When the voltage is high enough, in order to reach a new balance between interfacial tension, viscous friction and dielectric force, the LC droplet will be stretched outward along the electrodes. As a result, the incident beam will be deflected when it hits the stretched droplet's surface, leading to an increased attenuation, as Fig. 1(b) shows. Upon removing the voltage, the droplet will quickly return to its original state because of the interfacial tension.

3. Experimental results and discussion

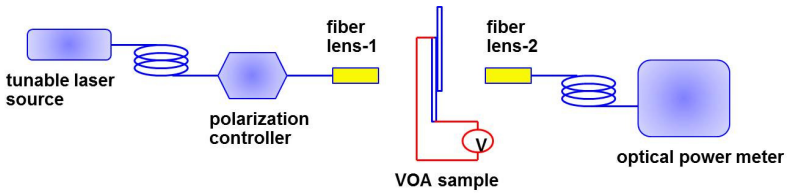

Fig. 2. Experimental setup for characterizing the VOA sample.

Figure 2 shows the experimental setup for characterizing our VOA sample. The free-space beam from a tunable laser light source (ANDO AQ4321D, λ = 1.52–1.62 μm) propagates through the input SMF. Its polarization state is manually adjusted by a fiber polarization controller (FPC560, Thorlabs). After being collimated by fiber lens-1, the beam propagates to fiber lens-2 which is connected to an output SMF. Finally, the output beam is monitored by an optical power meter (ANDO AQ8201-21). The fiber lenses are gradient index (GRIN) type devices enabling a near zero free-space-to-SMF coupling loss with the self-imaging configuration [26]. The distance between the two GRIN lenses was fixed at ~4 cm. The VOA sample was placed in vertical direction. At V = 0, the incident beam from lens-1 passes through the edge of the liquid droplet.

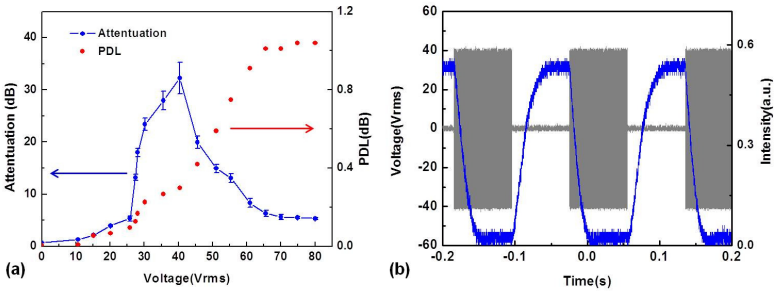

Fig. 3. Measured (a) Attenuation and PDL vs. operating voltages and (b) Switching time at V = $40V_{rms}$ (λ = 1550nm).

Figure 3(a) depicts the measured voltage-dependent attenuation and PDL of the VOA sample at 1550 nm. At V = 0, the beam propagated through the cell with ~0.7 dB insertion loss and ~0 dB PDL. As voltage increases, the attention first increases and reaches a maximum value of ~33 dB at V = 40.4 V_{rms}. Thus, the dynamic range is ~32 dB. As the voltage keeps increasing, the attenuation gradually decreases to ~5.32 dB at V = 80 V_{rms}. The reason for the observed phenomena is explained as follows. At V = 0, the incident beam stays aligned with the output SMF so that attenuation is the smallest (Fig. 4(a)). When the voltage is high enough, the LC droplet begins to stretch along the electrodes by the dielectric force. As a result, it gradually covers the incident beam. Instead of propagating through a pure silicone oil (L2) layer, the beam goes through the LC droplet and silicone oil sequentially. Due to the refractive index mismatch between these two liquids, the liquid-liquid interface deflects the incident beam away from the output SMF (Figs. 4(b)-4(c)). Thus, the attenuation increases accordingly, and it reaches maximum when the output beam is totally decoupled

#169848 - $15.00 USD Received 4 Jun 2012; revised 1 Jul 2012; accepted 5 Jul 2012; published 11 Jul 2012

from the output SMF (Fig. 4(d)). However, further increasing voltage will reduce the beam deflection and lower the attenuation, because extremely stretching the droplet will lead to a flatter liquid-liquid interface in the beam path (Figs. 4(e)-4(f)). From above discussion, we can see that the most effective working window for the proposed VOA is from Fig. 4(a) to Fig. 4(d).

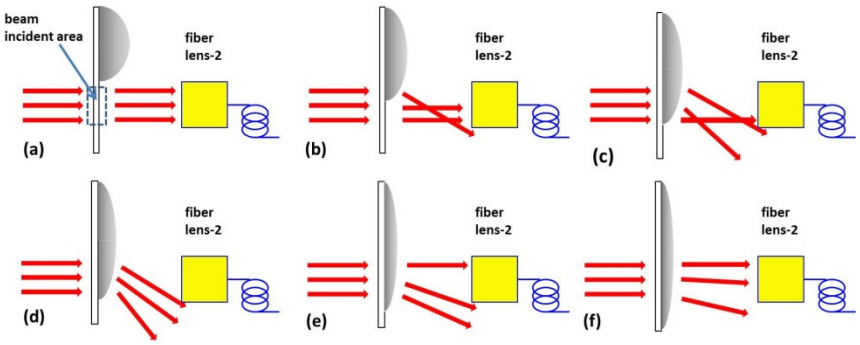

Fig. 4. Droplet surface stretching and beam deflection with increased voltage.

As a comparison, the PDL keeps increasing with the operating voltage consistently. It is ~0.3 dB at V = 40.4 V_{rms} and ~1 dB at V = 80 V_{rms}. PDL is induced by the birefringence effect of the LC material [27], and the acceptable PDL for VOAs should be less than 0.5 dB within the 0-10 dB attenuation range. As voltage increases, more LC molecules are reoriented along the electric field so that the PDL increases correspondingly. In the proposed VOA, the LC droplet is quite large (aperture D~450 μm, apex distance t~200 μm). Thus, even at 40V_{rms} only a very thin LC layer (near the bottom substrate) is affected by the electric fields, while the bulk LC molecules are still randomly oriented. Therefore, our device keeps a small PDL within the effective working window.

Figures 5(a)-5(c) show the broadband operation with an attenuation setting of 5 dB, 20 dB and 30 dB for the telecommunication C-Band (1530–1560 nm) respectively. The OSA (Optical Spectrum Analyzer) resolution is 10 dB/Div. The attenuation at a given voltage is quite inert to the operating wavelength. Figure 5(d) shows the broadband VOA operation for the attenuation settings at ~3 dB with a higher OSA resolution (2 dB/Div). The maximum in-band attenuation variation is measured to be ± 0.124 dB. The small oscillations of each curve may come from the Fabry-Perrot interference of the two substrate surfaces.

Response time is another important parameter for a VOA. Due to our facility limitation, instead of using the experimental setup shown in Fig. 2, we adopted a 1550nm laser diode (LAS DFB-1550, LaserMax), photo-receiver (Model 2031, New Focus) and oscilloscope (TDS 3032B, Tektronix) in our measurement. Response time was defined by the transmittance change between 10% and 90%. At 40 V_{rms} (500Hz) square voltage bursts, the fall (droplet stretching) and rise (droplet recovering) times were measured to be ~19.2 ms and 26.2 ms, respectively, as shown in Fig. 3(b). The cycle driving with two periods shows that the LC droplet returns to its original state quite well.

In our experiment, we intentionally let the incident beam pass the droplet's border, where a maximum change in the droplet's surface occurs. The purpose for doing so is to obtain large dynamic range and low peak operating voltage simultaneously. In the rest state, if the beam has already hit the LC droplet, then the insertion loss will be large. On the contrary, if the beam is too far from the droplet's border, then a higher voltage is required to reach the same dynamic range. The insertion loss can be reduced by using AR coating and high quality Teflon layer on the glass substrates. But it also depends on the coupling lenses. In practical applications, we may use V-groove in an etched silicon substrate to reduce the alignment complexity and lower the cost. The selected ZLI-4389 material with a high dielectric constant

#169848 - $15.00 USD Received 4 Jun 2012; revised 1 Jul 2012; accepted 5 Jul 2012; published 11 Jul 2012

and medium surface tension plays a key role in reducing the operating voltage. Otherwise, the droplet deformation will be very limited even under a high voltage [16,28,29]. To further decrease the operating voltage, interdigitated ITO electrodes with a smaller electrode gap can be considered. The dynamic range can be enlarged by adopting two liquids with a larger refractive index difference. The PDL can be further reduced by increasing the droplet size (especially the apex distance *t* of the droplet), but this will lead to a larger insertion loss since the cell gap is increased. The switching time is affected by the liquid interfacial tension and flow viscosity, and it can be improved by using a surrounding liquid with lower viscosity. To get a smoother attenuation curve, the device structure and driving scheme still need to be optimized.

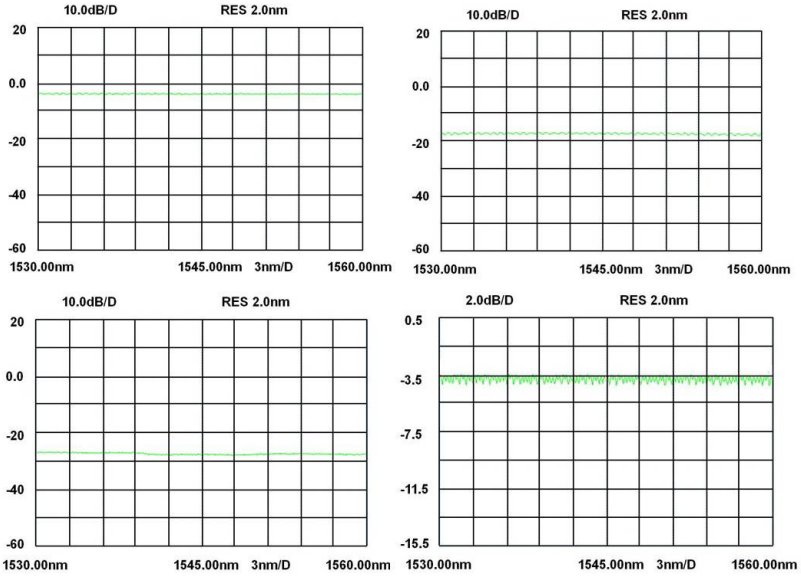

Fig. 5. Measured VOA broadband operation at (a) V = 25V_{rms} (~5dB attenuation setting), (b) V = 30V_{rms} (~20dB attenuation setting) and (c) V = 35V_{rms} (~30dB attenuation setting) for C-Band operation with OSA resolution of 10 dB/Div, and (d) V = 20V_{rms} (~3dB attenuation setting) with OSA resolution of 2 dB/Div.

4. Conclusion

We demonstrated a VOA based on dielectrically stretched LC droplet. The applied voltage stretches the LC droplet's surface, which in turn deflects the incident beam to decouple from the output SMF. Such a VOA provides competitive features like simple fabrication, broadband operation over C-Band, low insertion loss (~0.7 dB), large dynamic range (~32 dB), small PDL (~0.3d B), and low power consumption (~mW). Relatively low operating voltage (~40V_{rms}) and reasonably fast switching time (~20 ms) make this device promising for various photonic applications.

Acknowledgments

This work is partially supported by AFOSR under contract No. FA95550-09-1-0170.

#169848 - $15.00 USD Received 4 Jun 2012; revised 1 Jul 2012; accepted 5 Jul 2012; published 11 Jul 2012